

Supporting Information

Physicochemical studies of water-in-oil nonionic microemulsion in presence of benzimidazole-based ionic liquid and probing of microenvironment using model C-C cross coupling (Heck) reaction

Barnali Kar,[†] Soumik Bardhan,[†] Kaushik Kundu,[‡] Swapan Kumar Saha,[†] Bidyut K. Paul,[‡]

Sajal Das^{†*}

[†] Department of Chemistry, University of North Bengal, Darjeeling 734 013, India

[‡] Surface and Colloid Science Laboratory, Geological Studies Unit, Indian Statistical Institute, Kolkata 700 108, India [E-mail: bidyut.isical@gmail.com (Bidyut K. Paul)]

Authors for correspondence

Dr. Sajal Das

Department of Chemistry

University of North Bengal

Darjeeling-734 013, India

E-mail: sajal.das@hotmail.com

Phone: (91) (0353) -2776 -381

Fax: ((91) (0353)-2699 -001

Table of contents

1. Basics of the dilution method and thermodynamics of the transfer of cosurfactant from oil to the interface	3-6
2. Interfacial composition of water (or, IL)/Tween-20/Pn/Cy microemulsion in absence and presence of IL.....	6-8
3. Plots of n_a/n_s vs n_o/n_s (Fig. S1).....	8
4. Values of interfacial and thermodynamic parameters (TableS1).....	9
5. Plots of nonlinear dependence of $(\Delta G^0_{o \rightarrow i}/T)$ on $(1/T)$ (Fig. S2).....	10
6. Plots of conductivity and hydrodynamic diameter along with count rate (Fig. S3).....	11
7. Representative FTIR spectra of O-H band with deconvoluted curves (Fig. S4).....	12
8. Plots of the variation of different water species (Fig.S5).....	12
9. Base standardization of Heck reaction (Table S2).....	13
10. Mechanism of Heck reaction (Scheme S1).....	13
11. UV-Vis spectral analysis with the progress of reaction (Fig. S6).....	14
12. Plots of sample absorbance vs. volume of Pn (Fig. S7)	15
13. Spectral (^1H -NMR and ^{13}C -NMR) analysis of compounds	16
14. References	16-17

[A]. Basics of the dilution method and thermodynamics of the transfer of cosurfactant from oil to the interface

For a quaternary water-in-oil microemulsion system composed of water/ surfactant/cosurfactant /oil, the solubilization of water is governed by the distribution of cosurfactant molecules between oil and the interface at a fixed temperature. A small amount of cosurfactant may remain solubilized in the aqueous phase depending on its lipophilicity. A threshold amount of cosurfactant is required to stabilize a water-in-oil dispersion at a fixed molar ratio of water to surfactant (ω). As a result, an appropriate distribution constant (K_d) is attained, and governs cosurfactant molecules distributed between the interfacial region (consisting of surfactant molecules) and the oleic phase at a fixed temperature. The stable w/o microemulsion gets disrupted when excess oil is added and the system splits up into two distinct phases. Again, a threshold amount of cosurfactant is necessary to restore the w/o microemulsion equilibrium. This process is repeatedly followed in the dilution experiment. The concentrations of cosurfactant at the interface and in the bulk oil phase were estimated to get the distribution constant (K_d) by the dilution experiments in the light of the physicochemical rationale elaborated by Zheng et al.¹, Moulik et al.^{2,3}, Paul et al.⁴⁻⁶, and Abuin et al.⁷ The total number of moles of the cosurfactant, n_a present in the stable microemulsion is given by the relation,

$$n_a = n_a^i + n_a^w + n_a^o \text{-----(S1)}$$

where, n_a^i , n_a^w , n_a^o are the number of moles of cosurfactant in the interfacial, water and oil phases respectively. Since the solubility of cosurfactant in the oil is constant at a given temperature, the constant k_o can be written as

$$k_o = \frac{n_a^o}{n_o} \text{-----(S2)}$$

where n_o is the total number of moles of oil in the system. Combining Equations S1 and S2 we get

$$n_a = n_a^i + n_a^w + k_o n_o \text{-----(S3)}$$

Since the moles of cosurfactant in the interface and in the dispersed phase (water) depend on the surfactant concentration, Equation S3 may be converted into a more convenient form by dividing throughout by total number of moles of surfactant, n_s to give

$$\frac{n_a}{n_s} = \frac{n_a^i + n_a^w}{n_s} + k_o \frac{n_o}{n_s} \text{-----(S4)}$$

In our experiment, negligible water solubility of cosurfactant (Pn) leads to $n_a^w \approx 0$.⁵ Thus, above equation becomes,

$$\frac{n_a}{n_s} = \frac{n_a^i}{n_s} + k_o \frac{n_o}{n_s} \text{-----(S5)}$$

A plot of n_a/n_s against n_o/n_s should yield the values of the slope (S) and the intercept (I). Slope (S) is actually k_o and n_a^o can be determined from Equation S2. On the other hand, n_a^i can be calculated from the intercept (I), which is equal to n_a^i/n_s .

The partition of Pn between the continuous oil phase and the interface of the droplet can be expressed in terms of the distribution constant (K_d). K_d can be calculated from the ratio of mole fraction of Pn in the interfacial composition (X_a^i) to the mole fraction of Pn in the bulk oil phase (X_a^o),

$$K_d = \frac{X_a^i}{X_a^o} = \frac{n_a^i / (n_a^i + n_s)}{n_a^o / (n_a^o + n_o)} = \frac{n_a^i (n_a^o + n_o)}{n_a^o (n_a^i + n_s)} \text{-----(S6)}$$

Dividing numerator and denominator by $n_a^i n_a^o$, and putting the values of the slope (S) and the intercept (I) from Equation S5, we get

$$K_d = \frac{(1 + n_o/n_a^o)}{(1 + n_s/n_a^i)} = \frac{(1 + 1/S)}{(1 + 1/I)} = \frac{I(1 + S)}{S(1 + I)} \text{-----(S7)}$$

The standard Gibbs free energy change of transfer (ΔG^0_{o-i}) of Pn from the continuous oil phase to the interfacial region, between the water and oil, is obtained from the relation

$$\Delta G^0_{o-i} = -RT \ln K_d = -RT \ln \frac{X_a^i}{X_a^o} = -RT \ln \frac{I(1 + S)}{S(1 + I)} \text{-----(S8)}$$

The Gibbs-Helmholtz equation⁸ was used to get the standard enthalpy of the said transfer process of alkanol from oil to interface ($\Delta H^0_{o \rightarrow i}$). Thus,

$$[\partial (\Delta G^0_{o-i}/T) / \partial T]_p = - \Delta H^0_{o-i} / T^2 \text{----- (S9)}$$

Using chain rule of differentiation on the left hand side of equation (S9),

$$[\partial (\Delta G^0_{o-i}/T) / \partial T]_p = [\partial (\Delta G^0_{o-i}/T) / \partial (1/T)]_p [d(1/T)/dT] = [\partial (\Delta G^0_{o-i}/T) / \partial (1/T)]_p (-1/T^2) \text{----- (S10)}$$

Substituting this value into eqn. S(9) we get,

$$[\partial (\Delta G^0_{o-i}/T) / \partial (1/T)]_p (-1/T^2) = - \Delta H^0_{o-i} / T^2 \text{----- (S11)}$$

Hence⁸,

$$\Delta H^0_{o-i} = [\partial (\Delta G^0_{o-i}/T) / \partial (1/T)]_p \text{----- (S12)}$$

Herein, the $\Delta G^0_{o-i}/T$ vs. $1/T$ plots is nonlinear in nature in each case. Therefore, the points in $\Delta G^0_{o-i}/T$ vs. $1/T$ plots have been fitted in a 2⁰ polynomial equation as follows,

$$\Delta G^0_{o-i}/T = A + B (1/T) + C (1/T)^2 \text{(S13)}$$

Where, A, B and C are the polynomial coefficients.

The first derivation of equation (S13) produced the enthalpy ($\Delta H^0_{o \rightarrow i}$),^{2,3}

$$\Delta H^0_{o-i} = B + 2C^2 (1/T) \text{-----} \text{ (S14)}$$

Consequently, the corresponding entropy change (ΔS^0_{o-i}) can be found by the following relation,

$$\Delta S^0_{o-i} = (\Delta H^0_{o-i} - \Delta G^0_{o-i})/T \text{-----} \text{ (S15)}$$

The evaluation of standard specific heat capacity change of transfer process, $(-\Delta C^0_p)_{o-i}$, follows from the relation,

$$[(\Delta C^0_p)]_{o-i} = [\partial \Delta H^0_{o-i} / \partial T]_p \text{-----} \text{ (S16)}$$

The standard state herein considered is the hypothetical ideal state of the unit mole fraction.

[B]. Interfacial composition of water (or, IL)/Tween-20/Pn/Cy microemulsion in absence and presence of IL

The dilution method was employed for a nonionic surfactant, Tween-20-based w/o microemulsion system stabilized in Pn (cosurfactant) and Cy (oil) with varying IL content (= 0.0, 0.05, 0.10, 0.15 and 0.20 mol dm⁻³) at a fixed ω (= 30) and temperatures (293K→323K). From the data collected, graphs were constructed by plotting n_a/n_s against n_o/n_s according to Eq. (S5). Representative plots are illustrated in Figure S1. The plots were strikingly linear (average correlation of coefficients was 0.9965). From the Figure S1, the values of n_a^o and n_a^i were obtained from slopes (S) and intercepts (I), respectively and subsequently all the thermodynamic parameters [K_d , $\Delta G^0_{o \rightarrow i}$, $\Delta H^0_{o \rightarrow i}$, $\Delta S^0_{o \rightarrow i}$ and $(\Delta C^0_p)_{o \rightarrow i}$] were evaluated according to Eqs. (S1-S16).²⁻⁶ The values of above physicochemical parameters are presented in Table S1.

In order to underline the influence of IL content on the interfacial composition of Tween-20-based w/o microemulsion systems stabilized in Pn and Cy under various physicochemical conditions (mentioned earlier), n_a^i/n_s values [i.e. compositional variations of amphiphiles (both

Tween-20 and Pn) at the interface] are plotted against [IL] ($0.0 \rightarrow 0.20 \text{ mol dm}^{-3}$) and respective plots are depicted in Figure 1 (inset A). It has been observed from Figure 1 (inset A) that n_a^i values gradually increase with increase in [IL] at all temperatures with some exceptions at low and high temperatures (293 and 323K). The increase in n_a^i values may be attributed to the salting out of the polar head group of Tween-20 in the aqueous phase (i.e., nano water pool), resulting in enhanced interfacial packing of Tween-20 and Pn. Small and polarizable anion (Br^-) of 1-butyl-3-propyl benzimidazolium bromide tends to promote the water structure and dehydrate the ether oxygen of polyoxyethylene type nonionic surfactant (Tween-20 having 20 POE chains). Consequently, hydrophilicity of the surfactant (due to salting-out effect) decreases.⁹ Recently, it was reported that POE chains of Tween-20 produce electrostatic interaction with imidazolium cation, and thereby, stimulate the rigidity of IL/oil interface.^{10,11} Further, delocalization of the charge as well as the charge shielding due to the presence of both benzene and imidazolium ring in IL contribute the factor that influences the effective binding of Pn with IL and Tween-20 at the droplet surface. With increasing [IL], delocalization of charge will be more. Hence, requirement of Tween-20 molecules decreases at the interface, and consequently, Pn population (n_a^i) increases.¹² All these phenomena are responsible for observed increase in Pn population (n_a^i) at the interface with increase in [IL]. Similar results were also observed by Wang et al.¹³ for [bmim][BF_4]/Brij-35/1-butanol/toluene microemulsion with different $m_{\text{IL}}/m_{\text{H}_2\text{O}}$ values at different temperatures. On the other hand, n_a^i increases with increase in temperature in absence and presence of IL with some exceptions at higher [IL]. It can be explained on the basis of the interactions between the active constituents at the interfacial layer of the microemulsion (for example, hydrogen bonding interaction between IL-water, dipole-dipole or dipole-induced dipole interaction between Pn-Tween-20, and ion-dipole interaction between IL-Pn and IL-Tween-20)

(Scheme 1). With increase in temperature, all these interactions are diminished. Consequently, more Pn is accommodated at the interfacial layer, which imparts stability of the microemulsions.¹⁴ Similar behavior was also observed for both $[C_{12}mim]Br/1$ -pentanol/octane/ $[bmim][BF_4]$ systems¹³ and CTAB/alkanol/toluene/ $[bmim][BF_4]$ systems.¹⁵ No systematic trend as a function of IL content has been observed for n_a^o values (Table S1) at the studied temperature range.

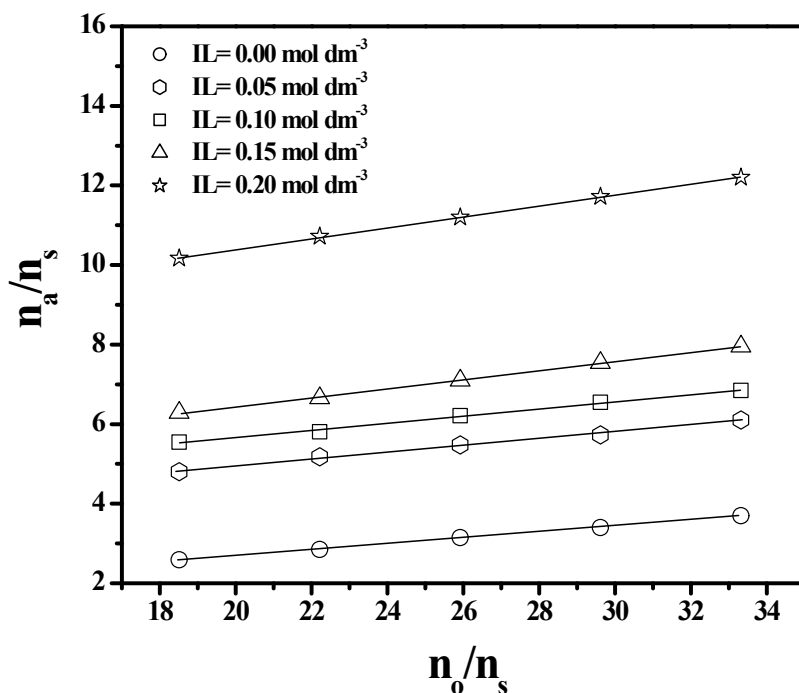


Figure S1. Plots of n_a/n_s vs. n_o/n_s according to Eq. (S4) for water/Tween-20/ pentanol /cyclohexane microemulsion system with different [IL] at $\omega = 30$ at constant temperature of 303K.

Table S1: Interfacial and bulk compositions of 1-pentanol, distribution constant (K_d) and thermodynamic parameters of its transfer from cyclohexane to the interface for w/o microemulsion containing 3.6 ml oil, 1 mmol of surfactant at constant ω ($= 30$) with varying [IL].

IL (mol dm ⁻³)	T(K)	$10^4 n_a^i$ (mol)	$10^3 n_a^o$ (mol)	K_d	$-\Delta G_{o \rightarrow i}^0$ (kJ mol ⁻¹)	$\Delta H_{o \rightarrow i}^0$ (kJ mol ⁻¹)	$\Delta S_{o \rightarrow i}^0$ (JK ⁻¹ mol ⁻¹)	$[\Delta C_p^0]_{o \rightarrow i}$ (kJ mol ⁻¹ K ⁻¹)
0.0	293	5.55	1.98	4.94	3.89	-32.58	-97.92	0.74
	303	5.82	1.23	7.81	5.18	-25.43	-66.83	
	313	9.34	1.25	9.35	5.82	-18.04	-39.03	
	323	9.99	1.00	11.79	6.63	-10.41	-11.69	
0.05	293	14.42	1.33	10.04	5.62	-11.70	-20.74	0.06
	303	16.18	1.41	9.76	5.74	-11.10	-17.69	
	313	16.46	1.00	13.57	6.79	-10.48	-11.80	
	323	17.10	1.07	13.94	6.86	-9.85	-9.25	
0.10	293	17.57	1.66	8.57	5.23	-14.15	-30.46	0.55
	303	18.95	1.57	9.21	5.59	-8.79	-10.56	
	313	18.03	1.07	13.01	6.68	-3.25	-10.97	
	323	18.12	1.15	12.7	6.70	2.48	28.42	
0.15	293	15.72	1.65	8.42	5.19	-4.07	3.82	-0.37
	303	20.8	1.90	7.88	5.20	-7.64	-8.07	
	313	22.28	1.23	11.85	6.43	-11.34	-15.69	
	323	17.75	1.15	12.09	6.69	-15.16	-26.21	
0.20	293	17.20	1.83	7.82	5.01	-0.4	15.73	-0.43
	303	39.55	2.16	7.72	5.15	-4.58	1.88	
	313	28.48	1.48	10.41	6.10	-8.89	-8.91	
	323	19.50	1.25	11.42	6.54	-13.34	-21.05	

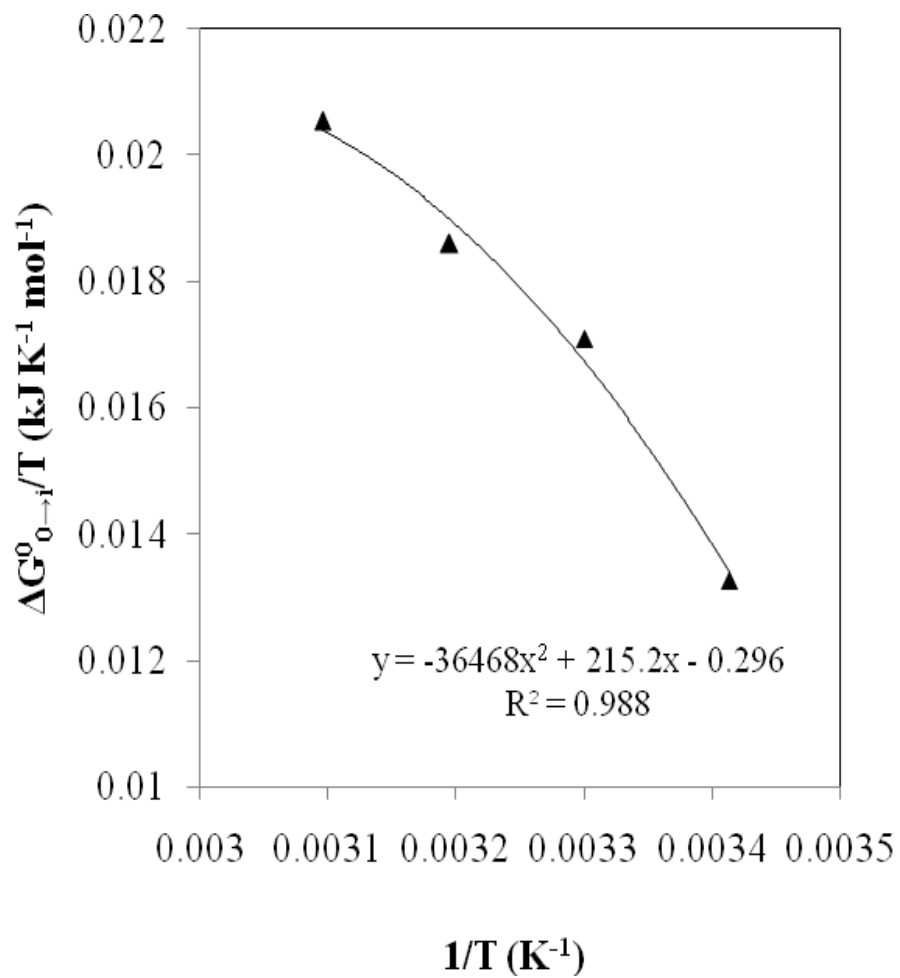


Figure S2. Plots of nonlinear dependence of ($\Delta G^0_{o \rightarrow i}/T$) on ($1/T$) in terms of a two degree polynomial equation for water/Tween-20/pentanol/cyclohexane microemulsion system in absence of IL at $\omega = 30$ with varied temperature (293K \rightarrow 323K).

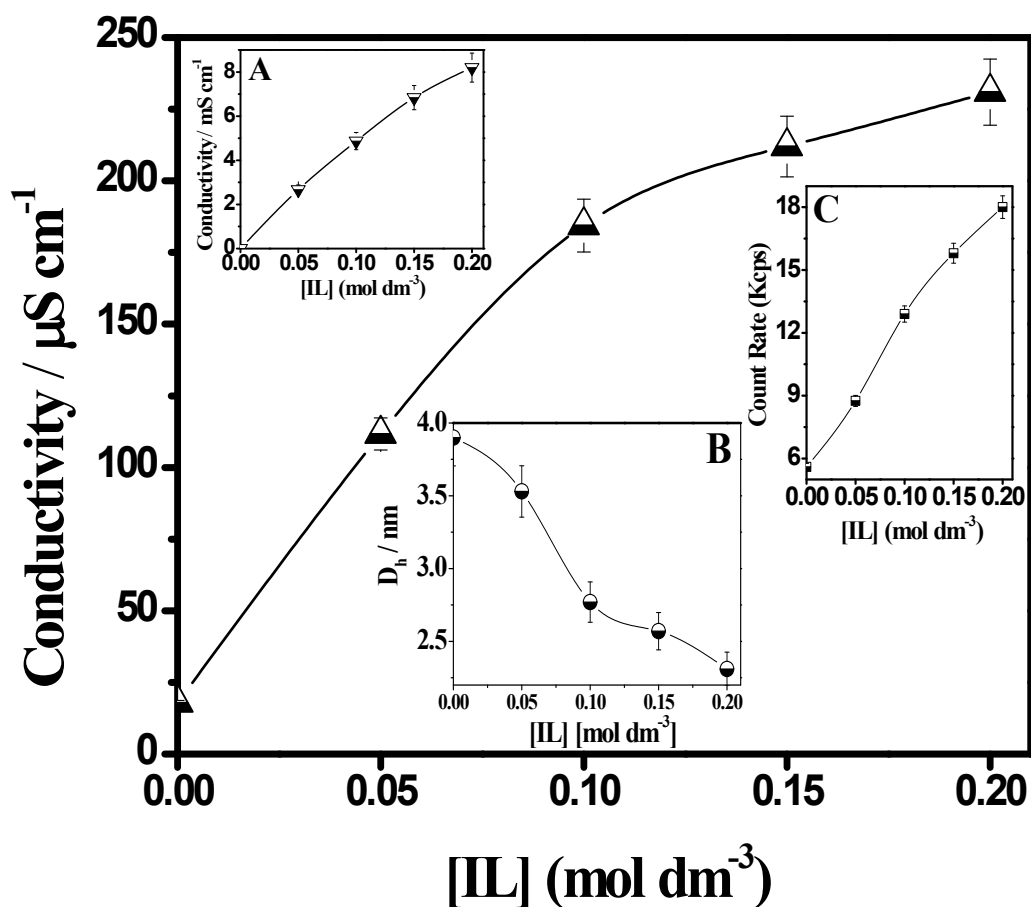


Figure S3. A representative plot for the variation of conductance as a function of IL content for water/Tween-20 /pentanol/cyclohexane microemulsion system at ω (= 30) and 303K. Inset A: Result of blank experiment (same concentration of IL in water). Inset B and C: Hydrodynamic diameter (D_h) (B) and Count Rate (C) of the microemulsion droplets for the same w/o systems with increasing IL content at identical condition.

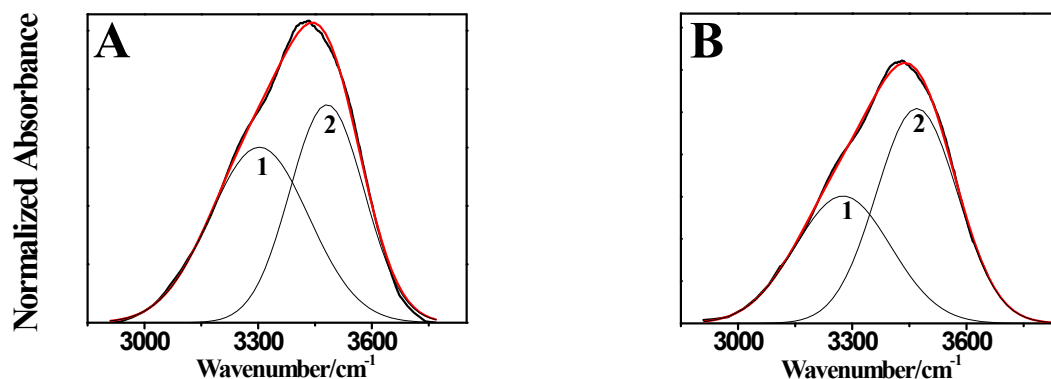


Figure S4: Representative FTIR spectra of O-H band for water/Tween-20/pentanol/cyclohexane microemulsion system at constant ω ($= 30$) and fixed temperature (303K). (A) In absence of IL and (B) in presence of $[IL] = 0.20 \text{ mol dm}^{-3}$. Specification: Experimental spectra (black curve), overall fitted curve (red) and deconvoluted curves (1: bulk water; 2: bound water).

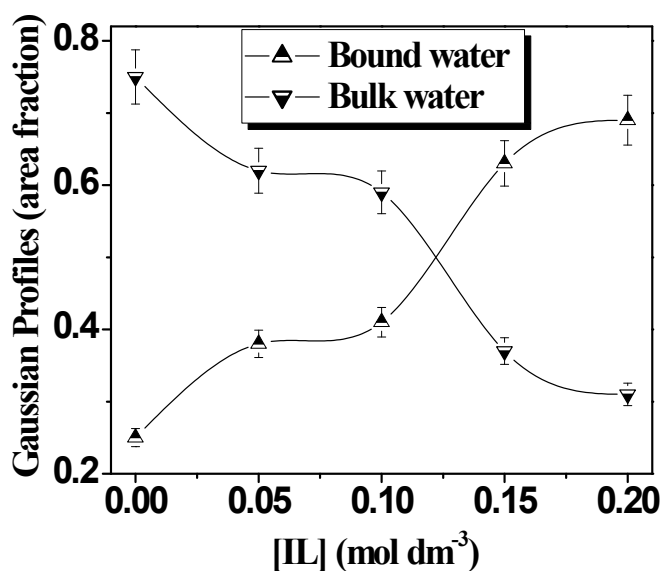
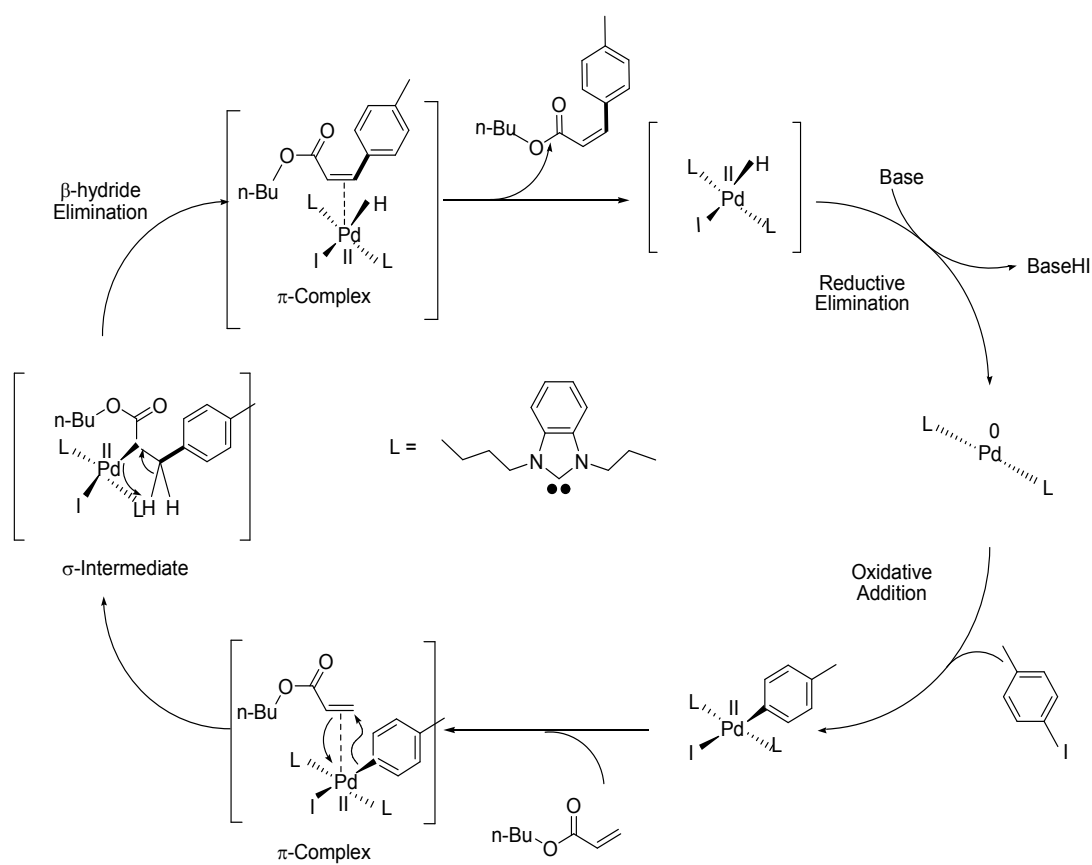


Figure S5. The variation of Gaussian profiles (area fraction) of the normalized spectra of different water species in water/Tween-20/pentanol/cyclohexane as a function of IL content.

Table S2. Heck coupling reaction in water (IL)/Tween-20/Pn/Cy microemulsion medium in presence of different bases at constant ω ($= 30$) and temperature (323K) ($[IL] = 0.05 \text{ mol dm}^{-3}$).

Entry	Base used	Time	Yield (%)
1	K ₂ CO ₃	1 hr.	30
2	NEt ₃	1 hr.	75
3	TMEDA	1 hr.	40



Scheme S1

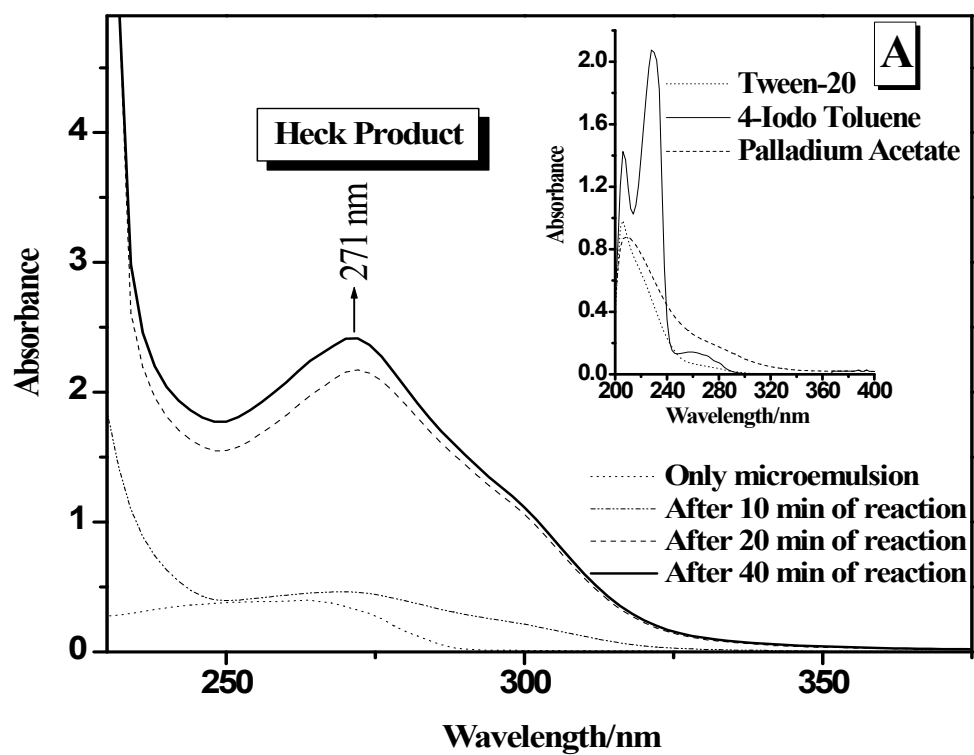


Figure S6. UV-Vis spectra of the water/Tween-20/Pn/Cy microemulsion system with the progress of reaction in presence of IL ($= 0.05 \text{ mol dm}^{-3}$). Inset A: UV-Vis spectra of individual component.

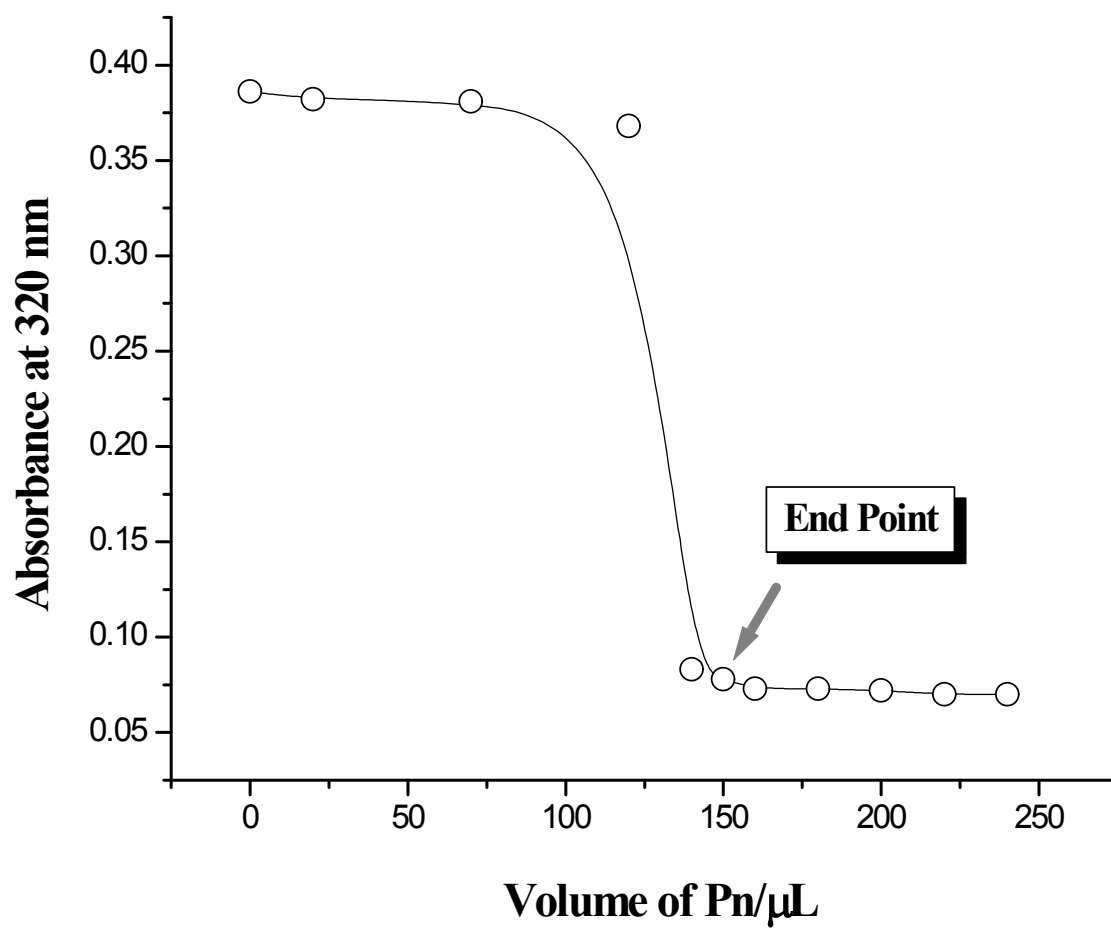


Figure S7. Plots of sample absorbance (measured at 320 nm) vs. volume of pentanol (Pn) for water/Tween-20/pentanol/cyclohexane microemulsion system at $\omega = 30$ and constant temperature of 303K .

[C]. Spectral analysis (^1H -NMR and ^{13}C -NMR)

1-Butyl-3-propylbenzimidazolium Bromide:

^1H -NMR (CDCl_3 , 300 MHz) δ 1.01-0.92 (m, 6H), 1.42-1.32 (m, 2H), 2.02-1.87 (m, 4H), 4.40-4.33 (m, 4H), 7.61 (s, 1H), 7.64 (s, 1H), 10.30 (s, 1H); ^{13}C -NMR (CDCl_3 , 75 MHz) δ 11.5, 14.2, 20.2, 24.5, 32.9, 50.5, 52.1, 123.3, 123.4, 137.3.

4-methyl butyl cinnamate:

^1H -NMR (CDCl_3 , 300MHz) δ 0.96 (t, 3H, $J = 7.2$ Hz), 1.44 (m, 2H), 1.68 (m, 2H), 2.36 (s, 3H), 4.20 (t, 2H, $J = 6.6$ Hz), 6.39 (d, 1H, $J = 16.2$ Hz), 7.18 (d, 2H, $J = 7.8$ Hz), 7.42 (d, 2H, $J = 7.8$ Hz), 7.66 (d, 2H, $J = 16.2$ Hz); ^{13}C -NMR (CDCl_3 , 75 MHz) δ 13.8, 19.2, 21.4, 30.8, 64.3, 117.2, 128.1, 129.6, 131.8, 140.6, 144.6, 167.3.

References:

1. O. Zheng, J-X. Zhao and X.-M. Fu, *Langmuir*, 2006, **22**, 3528-3532.
2. D. Mitra, I. Chakraborty, S.C. Bhattacharya, S.P. Moulik, S. Roy, D. Das and P.K. Das, *J. Phys.Chem. B*, 2006, **110**, 11314-11326.
3. K. Maiti, I. Chakraborty, S.C. Bhattacharya, A.K. Panda and S.P. Moulik, *J. Phys.Chem. B*, 2007, **111**, 14175-14185.
4. B.K. Paul and D.D. Nandy, *J. Colloid Interface Sci.*, 2007, **316**, 751-761.
5. K. Kundu, G. Guin and B. K. Paul, *J. Colloid Interface Sci.*, 2012, **385**, 96-110.
6. K. Kundu and B. K. Paul, *Colloid Polym. Sci.*, 2013, **291**, 613-632.
7. E. Abuin, E. Lissi and K. Olivares, *J. Colloid Interface Sci.*, 2004, **276**, 208-211.

8. Atkins' Physical Chemistry, P. Atkins, J. D. Paula, Oxford University Press, 2004, pp126.
9. R. K. Mitra and B. K. Paul, *J. Colloid and Interface Sci.*, 2005, **291**, 550-559.
10. S. Paul and A. K. Panda, *Colloids and Surfaces A: Physicochem. Eng. Aspects*, 2013, **419**, 113–124.
11. Y. Gao, L. Hilfert, A. Voigt and K. Sundmacher, *J. Phys. Chem. B*, 2008, **112**, 3711-3719.
12. S. Bardhan, K. Kundu, B. K. Paul and S. K. Saha, *Colloid Surfaces A*, 2013, **433**, 219-229.
13. F. Wang, Z. Zhang, D. Li, J. Yang, C. Chu and L. Xu, *J. Chem. Eng. Data*, 2011, **56**, 3328–3335.
14. J. Chai, L. Xu, W. Liu and M. Zhu, *J. Chem. Eng. Data*, 2012, **57**, 2394-2400.
15. Z. Zhang, F. Wang, D. Li and J. Yang, *J. Disp. Sci. Technol.*, 2012, **33**, 141-146.